

THE ANALYSIS OF BEARING-PAD TO PRESSURE-TUBE CONTACT HEAT TRANSFER EXPERIMENTS

T. NITHEANANDAN, Q.M. LEI, and R.G. MOYER

AECL Whiteshell Laboratories
Pinawa, Manitoba, Canada R0E 1L0

ABSTRACT

An experimental program was established to study the influence of hot bearing pads on temperature transients of a ballooning pressure tube under postulated loss-of-coolant accident conditions in a CANDU[®]. Twelve experiments were conducted in steam and Ar/O₂ environments. Measured temperature and power transients from the experimental program were used with the multipurpose code CATHENA Mod-3.4/Rev 7 to infer the contact heat transfer coefficient between the bearing pad and the pressure tube. The empirically derived contact conductances are of special interest in the safety analysis of CANDU reactors.

The contact heat transfer coefficients reached a maximum when the pressure-tube temperature was between 400 and 500°C beneath the bearing pads. The maximum value of contact heat transfer coefficient, calculated from experiments conducted in Ar/O₂ environments, ranged from 1.1 to 1.5 kW/(m²·K). In the steam environment the maximum value of contact heat transfer coefficient ranged between 1.0 to 4.5 kW/(m²·K).

The calculated contact heat transfer coefficients decreased to a negligible value (< 0.1 kW/(m²·K)) in all experiments once the pressure-tube temperature exceeded ~630°C. This drop in heat transfer coefficient was due to localized deformation of the pressure tube beneath the bearing pads caused by the localized hot spot and the internal pressure-tube pressure. This deformation resulted in deteriorating conformity, between the pressure tube and the bearing pad, as evidenced by a decrease in the pressure-tube heatup rate and a coincident increase in the bearing-pad heatup rate.

This paper summarizes the modeling methodology and analysis of results for the large-scale Integrated Bearing-Pad to Pressure-Tube Contact Heat Transfer experimental program. The work described in this paper was largely funded by the CANDU Owners Group (COG).

1. INTRODUCTION

In a CANDU (CANada Deuterium Uranium) reactor, bearing pads are brazed to the outer ring of the fuel bundles. The use of these bearing pads are two fold: first, they aid repeated movement of the bundle during online refuelling and two, they position the bundle concentrically in the pressure tube to maintain a uniform flow of liquid coolant around the bundle.

In the absence of liquid coolant in the fuel channel during some postulated large loss-of-coolant accident conditions, the bearing pads may contribute to a localized "hot spot" on the pressure tube. The transfer of decay heat from a fuel element in a voided channel occurs radially towards the pressure tube. The dominant mode of heat transfer between the fuel elements and the pressure tube is thermal radiation. In the vicinity of a bearing-pad, however, the contribution of conduction heat transfer will be a significant factor in addition to radiation. Heat is conducted

CANDU[®] is a registered trademark of Atomic Energy of Canada Limited (AECL).

between the bearing-pad and pressure-tube contacting surfaces through the interstitial gap gas and solid-to-solid contact. The magnitude or severity of the hot spot depends largely on the overall bearing-pad to pressure-tube contact conductance. Therefore, the bearing-pad to pressure-tube contact conductance is of special interest for safety analysis of the fuel channel.

Two broad categories of experiments, namely the single effect and integrated effect tests, were conducted to determine the bearing-pad to pressure-tube contact conductance. The single effects tests obtained experimental data from a small scale experimental apparatus [1,2,3]. The integrated effects tests were conducted in an apparatus that consisted of full diameter pressure tube and calandria tube and representative fuel bundle [4].

Sixteen single effect tests were performed in total. These tests used a 40 mm by 50 mm section of Zr-2.5 Nb pressure tube and a single 50-mm long simulated fuel element pin in Argon, Vacuum and Ar/O₂ environments. Tests were performed in steady and transient states. From steady-state vacuum tests, the solid-to-solid component of the bearing-pad to pressure-tube contact heat transfer coefficient was obtained. Knowing the solid-to-solid component, and repeating the steady-state tests in Ar/O₂ environment, the interstitial gas conduction component was obtained from the difference between the heat transfer coefficients, obtained in Ar/O₂ and vacuum tests. Conversion factors were derived as a function of interstitial gas temperature using the solid-to-solid and interstitial gas conduction components of the contact heat transfer coefficient. These conversion factors were required to convert the transient state contact heat transfer coefficients obtained in Ar/O₂ environment to a reactor-typical D₂O environment.

The single effect transient-state experimental data of DeVaal et al. [1] and Krause et al. [3] were analysed using the finite element codes ABAQUS and ANSYS to estimate the bearing-pad to pressure-tube contact conductance. The various analyses [1,2,3] showed a three-step change in the contact conductance between the bearing pad and its pressure tube. For bearing-pad to pressure-tube interface temperatures below 550°C, the contact conductance was between 0.5 kW/(m²·K) and 1 kW/(m²·K) in an Ar/O₂ environment. At an interface temperature between 550°C and 800°C, the contact conductance increased from 1 to between 2.5 and 5 kW/(m²·K). The contact conductance varied widely above an interface temperature of 800°C, reaching 12 to 14 kW/(m²·K) in some tests while remaining below 5 kW/(m²·K) in others.

In some of the single effect tests, a uniaxial tensile load was applied via a set of grips to simulate the hoop strain in a pressure tube during ballooning. Although this method was appropriate in simulating the hoop strain, it was not appropriate to simulate the radial movement of a pressure tube during ballooning. The influence radial movement of the pressure-tube has on contact heat transfer (during ballooning) became apparent when the analysis of the large scale integrated tests revealed a decrease in the pressure tube heatup rates once the pressure tube reached a threshold temperature above 630°C [4]. As the heatup rate of the pressure tube decreased, the bearing-pad heatup rate increased simultaneously. This trend was due to deteriorating conformity between the bearing-pad and the pressure-tube surfaces.

An analysis of the integrated effects tests using CATHENA was initiated to obtain the transient bearing-pad to pressure-tube contact conductance values which would reflect the radial, circumferential and axial displacement of the pressure tube during ballooning. The objective of the present analysis was to empirically determine the spectrum of bearing-pad to pressure-tube contact conductance of all twelve integrated tests.

2. THE LARGE SCALE INTEGRATED EXPERIMENTS

2.1 Experimental Apparatus

The integrated effect bearing-pad to pressure-tube heat transfer tests were documented by Moyer et al. [4]. A short description of the salient features of these tests are given below.

THE ANALYSIS OF BEARING-PAD TO PRESSURE-TUBE CONTACT HEAT TRANSFER EXPERIMENTS

T. NITHEANANDAN, Q.M. LEI, and R.G. MOYER

AECL Whiteshell Laboratories
Pinawa, Manitoba, Canada R0E 1L0

ABSTRACT

An experimental program was established to study the influence of hot bearing pads on temperature transients of a ballooning pressure tube under postulated loss-of-coolant accident conditions in a CANDU®. Twelve experiments were conducted in steam and Ar/O₂ environments. Measured temperature and power transients from the experimental program were used with the multipurpose code CATHENA Mod-3.4/Rev 7 to infer the contact heat transfer coefficient between the bearing pad and the pressure tube. The empirically derived contact conductances are of special interest in the safety analysis of CANDU reactors.

The contact heat transfer coefficients reached a maximum when the pressure-tube temperature was between 400 and 500° C beneath the bearing pads. The maximum value of contact heat transfer coefficient, calculated from experiments conducted in Ar/O₂ environments, ranged from 1.1 to 1.5 kW/(m² · K). In the steam environment the maximum value of contact heat transfer coefficient ranged between 1.0 to 4.5 kW/(m² · K).

The calculated contact heat transfer coefficients decreased to a negligible value (< 0.1 kW/(m² · K)) in all experiments once the pressure-tube temperature exceeded ~630° C. This drop in heat transfer coefficient was due to localized deformation of the pressure tube beneath the bearing pads caused by the localized hot spot and the internal pressure-tube pressure. This deformation resulted in deteriorating conformity, between the pressure tube and the bearing pad, as evidenced by a decrease in the pressure-tube heatup rate and a coincident increase in the bearing-pad heatup rate.

This paper summarizes the modeling methodology and analysis of results for the large-scale Integrated Bearing-Pad to Pressure-Tube Contact Heat Transfer experimental program. The work described in this paper was largely funded by the CANDU Owners Group (COG).

1. INTRODUCTION

In a CANDU (CANada Deuterium Uranium) reactor, bearing pads are brazed to the outer ring of the fuel bundles. The use of these bearing pads are two fold: first, they aid repeated movement of the bundle during online refuelling and two, they position the bundle concentrically in the pressure tube to maintain a uniform flow of liquid coolant around the bundle.

In the absence of liquid coolant in the fuel channel during some postulated large loss-of-coolant accident conditions, the bearing pads may contribute to a localized "hot spot" on the pressure tube. The transfer of decay heat from a fuel element in a voided channel occurs radially towards the pressure tube. The dominant mode of heat transfer between the fuel elements and the pressure tube is thermal radiation. In the vicinity of a bearing-pad, however, the contribution of conduction heat transfer will be a significant factor in addition to radiation. Heat is conducted

CANDU® is a registered trademark of Atomic Energy of Canada Limited (AECL).

between the bearing-pad and pressure-tube contacting surfaces through the interstitial gap gas and solid-to-solid contact. The magnitude or severity of the hot spot depends largely on the overall bearing-pad to pressure-tube contact conductance. Therefore, the bearing-pad to pressure-tube contact conductance is of special interest for safety analysis of the fuel channel.

Two broad categories of experiments, namely the single effect and integrated effect tests, were conducted to determine the bearing-pad to pressure-tube contact conductance. The single effects tests obtained experimental data from a small scale experimental apparatus [1,2,3]. The integrated effects tests were conducted in an apparatus that consisted of full diameter pressure tube and calandria tube and representative fuel bundle [4].

Sixteen single effect tests were performed in total. These tests used a 40 mm by 50 mm section of Zr-2.5 Nb pressure tube and a single 50-mm long simulated fuel element pin in Argon, Vacuum and Ar/O₂ environments. Tests were performed in steady and transient states. From steady-state vacuum tests, the solid-to-solid component of the bearing-pad to pressure-tube contact heat transfer coefficient was obtained. Knowing the solid-to-solid component, and repeating the steady-state tests in Ar/O₂ environment, the interstitial gas conduction component was obtained from the difference between the heat transfer coefficients, obtained in Ar/O₂ and vacuum tests. Conversion factors were derived as a function of interstitial gas temperature using the solid-to-solid and interstitial gas conduction components of the contact heat transfer coefficient. These conversion factors were required to convert the transient state contact heat transfer coefficients obtained in Ar/O₂ environment to a reactor-typical D₂O environment.

The single effect transient-state experimental data of DeVaal et al. [1] and Krause et al. [3] were analysed using the finite element codes ABAQUS and ANSYS to estimate the bearing-pad to pressure-tube contact conductance. The various analyses [1,2,3] showed a three-step change in the contact conductance between the bearing pad and its pressure tube. For bearing-pad to pressure-tube interface temperatures below 550°C, the contact conductance was between 0.5 kW/(m²·K) and 1 kW/(m²·K) in an Ar/O₂ environment. At an interface temperature between 550°C and 800°C, the contact conductance increased from 1 to between 2.5 and 5 kW/(m²·K). The contact conductance varied widely above an interface temperature of 800°C, reaching 12 to 14 kW/(m²·K) in some tests while remaining below 5 kW/(m²·K) in others.

In some of the single effect tests, a uniaxial tensile load was applied via a set of grips to simulate the hoop strain in a pressure tube during ballooning. Although this method was appropriate in simulating the hoop strain, it was not appropriate to simulate the radial movement of a pressure tube during ballooning. The influence radial movement of the pressure-tube has on contact heat transfer (during ballooning) became apparent when the analysis of the large scale integrated tests revealed a decrease in the pressure tube heatup rates once the pressure tube reached a threshold temperature above 630°C [4]. As the heatup rate of the pressure tube decreased, the bearing-pad heatup rate increased simultaneously. This trend was due to deteriorating conformity between the bearing-pad and the pressure-tube surfaces.

An analysis of the integrated effects tests using CATHENA was initiated to obtain the transient bearing-pad to pressure-tube contact conductance values which would reflect the radial, circumferential and axial displacement of the pressure tube during ballooning. The objective of the present analysis was to empirically determine the spectrum of bearing-pad to pressure-tube contact conductance of all twelve integrated tests.

2. THE LARGE SCALE INTEGRATED EXPERIMENTS

2.1 Experimental Apparatus

The integrated effect bearing-pad to pressure-tube heat transfer tests were documented by Moyer et al. [4]. A short description of the salient features of these tests are given below.

The experimental apparatus was a 1.2-m long section of Zr-2.5 Nb pressure tube placed inside a 1.1-m long Zr-2 calandria tube (Figure 1a). The calandria tube was submerged inside an open tank containing stagnant water heated to a temperature of 74°C. The water level above the top surface of the calandria tube was at least 250 mm.

The electrically heated FES bundle had 16 elements to simulate the outer ring of a typical 28-element CANDU fuel bundle (Figures 1b). The bearing-pads and spacer pads were spot welded to the FES sheath (15.2-mm OD and 14.4-mm ID, Zr-4) at five axial locations (Figure 1a). One ring of bearing-pads was located at the centre of the test section. The remaining four rings were located on either side of the central bearing pad location: two bearing-pad rings 197 mm from the centre and another two rings 394 mm from the centre. All bearing pads at the central bearing-pad ring were brazed to the FES sheath such that the heat transfer coupling between the sheath and the bearing pad would be typical to that in CANDU fuel bundles. Tungsten weight cans were placed inside of the FES ring to represent the weight of a CANDU fuel bundle. The mass per unit length of a typical FES bundle was 49.4 g/mm.

Three different types of bearing pads were used during the tests. Regular bearing pads (deemed "as received") were used in all experiments except for tests 8 and 9. In test 8, the bearing pads at the central bearing-pad ring were abraded to simulate the wear occurring in reactor during operation. Test 9 used modified "T"-type bearing pads designed to reduce the crevice corrosion around the bearing pad of in-reactor fuel bundles.

All 16 FESs were connected in parallel to a 5000 A DC power source. The temperature field was measured by 53 thermocouples placed at suitable locations in the test section. Two thermocouples measured the water temperature surrounding the calandria tube 40 mm above and 40 mm below the test section along the centreline. Two more resistance temperature detectors measured the tank water temperature. Linear Variable Differential Transformers (LVDT) monitored the relative displacement between the pressure tube and the calandria tube at the top and bottom. A second LVDT at the bottom was located 104 mm from the centreline along the bottom of the channel to monitor displacement of the pressure tube between bearing-pad rings (Figure 1a).

In tests 1 to 4, the pressure tube was filled with distilled water at the beginning of each test (Table 1). A total of 3.31 liters was required to completely fill the channel and associated pipes. In these four tests, the bottom seven FESs were turned on at low power to preheat the test section. As the water temperature approached 100°C, the volume increase was vented through the top of the pressure tube. After the water in the pressure tube started to boil, the top valve was closed and the bottom valve was opened to drain the water. As the bottom seven FESs slowly heated the pressure tube to 300°C the bottom valve was closed and the hydraulic pressure-control valve was opened to increase the pressure-tube pressure. When the pressure reached the desired level, all 16 FESs were connected to the power supply and electric power to the test section was ramped to a predetermined value to start the test.

In tests 5 to 12 various preheating strategies were tried to minimize the top-to-bottom temperature difference caused by free convection. The pressure tube was preheated by applying power to the bottom FESs. When the bottom pressure-tube temperatures were about 30°C hotter than the top, power was supplied to all FESs. After this initial preferential heating of the pressure tube, all 16 FESs were connected to the power supply and electric power to the test section was ramped to a predetermined value to start the test.

2.2 Experimental Results

Uncertainties in the temperature measurements were obtained from in-house calibrations and from manufacturer's specifications. All thermocouples used in the experiment were standard grade. Type-R thermocouples were used on FES and bearing-pad surfaces with the following uncertainty ranges:

below 600°C
600°C to 1300°C

(±4.5°C) + (±0.25%), and
±0.65%.

Pressure-tube temperatures were monitored using Type-K thermocouples which had the following uncertainty ranges.

below 300°C	(±2.2°C) + (±0.25%), and
300°C to 1000°C	±1.0%.

Typical estimated uncertainties in pressure measurements were ±0.3%. The estimated uncertainty in the total measured power was ±4.6% during the experiment. The electric power lost to the bus bars and connections was estimated to be 1% of the power supplied to the bundle.

In these experiments pressure-tube internal pressure, pressure-tube heating rate, the power to the FES bundle, and water subcooling were controlled (Table 1). For each test, the test section was pressurized and the power increased to the desired level. The test section pressure and the temperature of the instrumented section were recorded by a data acquisition system. The test was terminated once the pressure tube ballooned in to contact with the calandria tube.

3. ANALYSES OF INTEGRATED EXPERIMENTS USING CATHENA Mod-3.4/Rev 7

The analyses of the integrated tests were conducted using CATHENA Mod-3.4/Rev 7 code. CATHENA is a one-dimensional thermalhydraulics computer code developed at Whiteshell Laboratories for the analysis of postulated loss-of-coolant accident scenarios in CANDU reactors [5]. CATHENA has the ability to model a reactor channel in detail. The thermal responses of individual fuel pins, the pressure tube and the calandria tube can be simulated in the axial, radial, and circumferential directions simultaneously. As well, the thermal effects of contacting metal surfaces can be modeled.

The rate of heat transfer across two contacting surfaces is determined by the thermal contact conductance and the temperature difference between the two surfaces. The thermal contact conductance (h_{CC}) per unit area of an interface of area (A), across which a temperature drop (ΔT) exists, is defined by

$$h_{CC} = Q/(A \Delta T) \quad (1)$$

where Q is the total rate of heat flow. The area (A) is the projected area of a bearing pad. The temperature difference across the interface (ΔT) is the calculated temperature difference between the two contacting surfaces.

3.1 Analytical Procedure

A detailed description of the analytical procedure is given in Reference [6]. A brief description of the procedure is provided here for completeness.

In this analysis two independent variables were identified, the contact conductance and the emissivity of fuel sheath. Two CATHENA models were developed to determine these two independent variables for each experiment. The first model, model A, estimated the surface emissivity of the FES as a function of time while the second model, model B, estimated the contact conductance between the bearing pad and the pressure tube. Model A used the experimental data obtained from the mid-plane between bearing-pad rings where radiation heat transfer was the dominant mode of heat transfer. Model B used the experimental data obtained from the central bearing-pad ring and assumed the estimated emissivities from model A for the radiation heat transfer calculations.

A flow chart outlining the procedure adopted in determining transient bearing-pad to pressure-tube contact conductance is given in Figure 2. The flow chart illustrates how converged solutions were obtained from the respective models.

The objective of the CATHENA calculation using model A was to determine if the assumed emissivities produced the same FES surface temperature (T_{FES}) as in the experiment. Sensitivity studies showed that the influence of emissivities of the stainless steel weight cans (ϵ_{SS}) and pressure tube (ϵ_{PT}) have on estimated FES surface temperatures was insignificant compared to the effect of the FES surface emissivities (ϵ_{FES}). Therefore, suitable emissivities were selected for the pressure tube ($\epsilon_{PT} = 0.75$) and stainless steel weight can ($\epsilon_{SS} = 0.3$) from the literature [7]. Only the emissivity of the FES sheaths was assumed to change. These transient values were calculated using model A. The procedure illustrated in Figure 2 was:

1. The measured pressure-tube temperatures between bearing-pad rings were supplied to model A as prescribed boundary conditions.
2. Model A was run with assumed values of FES emissivity during the transient.
3. The calculated ($T_{FES,pr}$) and measured FES surface temperatures were compared, the FES emissivity in the code was adjusted accordingly and model A was rerun.
4. This procedure was repeated until convergence between the experimental and the calculated temperatures was achieved. The results were considered converged when the difference between measured and calculated FES temperatures was less than 30°C .

The second model, model B, determined the contact conductance at the central bearing-pad location. The emissivities from model A were supplied to model B. Model B was then used to determine the bearing-pad to pressure-tube contact conductance.

The calculation procedure while running model B was:

1. The measured pressure-tube temperatures from the central bearing pad location were supplied to model B as prescribed boundary conditions.
2. The measured and calculated bearing-pad temperatures were supplied as an input signal to the control device model.

3.2 Modeling Assumptions

The geometry considered in this analysis was a 1/16th sector of the FES bundle (22.5° included angle), shown in Figure 1b. The geometry was further divided circumferentially into the following sub-sectors: tungsten weight can into three equal sub-sectors, the semi-circular FES pins into nine equal sub-sectors, and the pressure tube into ten equal sub-sectors.

The number of nodes in the radial direction used in both models was selected to ensure efficiency and accuracy of the calculations. The tungsten weight can, FES, and pressure tube were given 11 radial nodes each. The bearing pads were assigned six radial nodes each. Increasing the number of radial nodes further had no significant influence on the calculated results.

Heat transfer within the 1/16th sector was assumed to be two dimensional (radial and circumferential). Heat transfer in the axial direction was assumed negligible. The outside circumference of the pressure tube was assigned measured pressure-tube temperatures which reflect the effect of three-dimensional heat transfer in the experiments. The pressure-tube temperatures between the thermocouple locations, along the circumferential direction, were linearly interpolated. Symmetry was assumed across the two radial boundaries separating the geometry shown in Figure 1b.

An 8-mm long axial section of the fuel bundle, passing through the axial central plane of the bearing pad, was used in this analysis. This section was approximately 1/3 of the bearing-pad length. The heat transfer calculation was independent of the axial length selected, as axial heat flow was assumed negligible. Since the volume of the bearing pad was small relative to the FES, the influence of the bearing-pad discontinuity at the edges was expected to be small on the thermal behaviour of the pressure tube or the FES.

The radiation heat transfer amongst the various surfaces was modeled using a two-dimensional view factor matrix. All radiant surfaces were treated to be opaque, diffuse, grey, and surrounded by a nonabsorbing and nonscattering medium.

The fuel element simulator was modeled in detail. Experimental power history was applied uniformly in the 6-mm diameter graphite rod. A 0.06-mm helium gas gap was modeled between the graphite rod and the alumina insulation pellet and between the alumina insulation pellet and the Zr-4 cladding.

Temperature-dependent conductance (thermal conductivity of Helium divided by the gas gap distance) and radiation were used to model the two-dimensional heat flow from the heated graphite rod to FES cladding. The collapse of FES cladding at high temperatures, due to the 1 MPa differential pressure between the outside and inside surfaces of the FES cladding, was neglected in the calculation.

Thermal conductivity, density and specific heat of tungsten, insulating cement, and alumina were obtained from references [8] and [9]. The properties of Ar, O₂, ZrO₂, zircaloy, stainless steel, and graphite were obtained from the internal property tables available in CATHENA.

3.3 Modeling Results and Discussion

The increase in emissivity of the FES sheath during the experiments is attributed to the combined effect of zirconium sheath oxidation and the dependence of emissive power on temperature.

The validity of Model A, as a suitable method of calculating the FES sheath emissivity, was verified by comparing the calculated emissivities with the oxide thickness method [10]. A comparison of the two methods demonstrated that the empirical approach used in Model A compares satisfactorily with the emissivities calculated by the oxide layer thickness method.

In all tests, except test 1, the emissivities were first determined using model A. The emissivity transients so determined were then applied to model B during the analysis of contact heat transfer. In test 1, the FES-cladding and pressure-tube temperatures were not monitored at the mid point between bearing pad location. Thus test 1 was excluded from this study.

3.3.1 Contact Conductance

Once the thermal-radiation-heat transfer was adequately characterised, the next step was to characterize the bearing-pad to pressure-tube contact heat transfer. The emissivities calculated using Model A for each test were supplied to the corresponding model B of the same test.

In this analysis, the measured pressure-tube temperatures were used as a prescribed boundary condition and a comparison of measured and calculated bearing-pad temperatures were used as a measure of convergence.

Figures 3 and 4 show the contact conductance required to achieve good agreement between the calculated and measured bearing-pad temperatures in tests 3 and 12. Because of the large thermal inertia of FESs, compared to the thermal inertia of bearing pads, the FES temperature did not respond to rapid changes in contact heat transfer. The changes in the bearing-pad heatup rates reflected the changes in contact conductance more directly than the changes

in FES temperature. Therefore, the calculated temperatures were more closely matched to the measured bearing-pad temperature than the FES sheath temperatures.

The contact conductances reported in this report were an average contact conductances for the projected area of a bearing pad. It is important to recognize the influence of local surface conditions, especially the metallographic surface profile and the strain induced deformations, on the calculated contact conductance [3]. Although no attempt was made in this study to classify the metallographic surface profiles of the pressure tube or the bearing pad, the results were deemed to adequately include these effects because:

- a) readings of the thermocouples on the pressure tube, bearing pad and FES thermally responded to variations in the microscopic and macroscopic surface conditions, and therefore the measured temperature difference ($\Delta T_{\text{measured}}$) implicitly contained the information on local surface conditions; and
- b) the derived bearing-pad to pressure-tube contact conductance, $h_{\text{CC}} (Q/\Delta T_{\text{measured}})$ thus represents the overall thermal behaviour of the two contacting surfaces.

Table 2 summarizes the test results which were grouped based on the pressurizing medium used in the test. The initial contact conductances in the steam tests (series 1, tests 2, 3 and 4) were approximately two to three times larger than in the Ar/O₂ tests. In the steam tests, the initial contact heat transfer coefficient ranged between 1.1 and 6.8 kW/(m² · K). In comparison, the initial contact heat transfer coefficient in the Ar/O₂ tests ranged between 0.05 and 2.1 kW/(m² · K). The differences between the steam and Ar/O₂ tests existed because the contact conductance was significantly influenced by the interstitial gap material during the initial heatup phase. Since the temperatures of the contacting surfaces were low during this initial heatup period, the surface microhardness of the pressure-tube and bearing-pad materials did not change appreciably. However, in the steam tests some condensate remained trapped inside the interstitial gap between the bearing pad and the pressure tube at the start of the tests. As the thermal conductivity of liquid water at a saturation pressure of 3.2 MPa is 14 times larger than the thermal conductivity of water vapour, a higher contact heat transfer coefficient existed in the early stages of the steam tests. The high contact heat transfer coefficients decreased once the trapped liquid inside the gap boiled off.

In the Ar/O₂ tests (series 2, tests 5 - 12), except for test 6, the initial contact heat transfer coefficient ranged between 0.05 to 0.6 kW/(m² · K). In Test 6, the contact heat transfer coefficient was observed initially to be 2.1 kW/(m² · K), but decreased to 1.1 kW/(m² · K) within 5 s of the start of the transient. Such a high initial contact heat transfer coefficient for a short period of time was probably caused by good metal to metal contact between the contact surfaces.

The maximum contact heat transfer coefficient shown in Table 2 occurred when the pressure tube had reached approximately 400 - 500 °C. The enhanced contact heat transfer at these temperatures, prior to significant ballooning, were likely due to microstructural changes between the contacting surfaces. Two material properties influenced the microstructural changes and, subsequently, the contact heat transfer. These were surface hardness and the yield point of the contacting surfaces. At the interface between two surfaces, the solids are in contact at discrete points. When the metals were heated, the hardness of the material decreased due to plastic deformation, increasing metal-to-metal contact areas and increasing the bearing-pad to pressure-tube contact conductance. The increase in contact conductance due to the reduction in surface hardness occurs prior to significant ballooning.

The maximum values of the calculated contact heat transfer coefficients, obtained from all Ar/O₂ tests, are shown in Figure 5a as a function of interfacial temperature. The interfacial temperature is defined as the average between the calculated bearing-pad surface temperature and the calculated pressure-tube surface temperature at the contacting interface. The maximum contact heat transfer coefficients remained between 1 and 1.5 kW/(m² · K) up to an interfacial temperature of 750 °C. The heat transfer coefficient generally decreased to a negligible value at an interfacial temperature of 850 °C for test pressures ranging from 3 to 6 MPa, but in the experiment where the internal pressure was 1 MPa, the drop in contact heat transfer coefficient occurred at an interfacial temperature of 950 °C.

The maximum contact heat transfer coefficient, calculated during the middle of the transient, among the three steam tests was 4.5 kW/(m²·K) (Test 3). The maximum contact heat transfer coefficient in the Ar/O₂ tests ranged from 1.1 to 1.5 kW/(m²·K), except in test 6 where the maximum was 2.0 kW/(m²·K) for a brief period of 2 s. The thermal conductivity of steam (H₂O) is approximately twice that of the Ar/O₂ gas [2]. Therefore, the maximum contact heat transfer coefficients calculated in the steam tests is expected to be twice that of Ar/O₂ tests [2]. A comparison between the two maximums revealed that they were in the same order of magnitude as calculated by the ratio of the two conductivities.

After the initiation of pressure tube ballooning, the contact conductance consistently dropped to a negligible value in all tests as shown by a drop in the pressure tube heatup rate and increase in bearing-pad temperatures during ballooning. Figures 3a and 4a show a comparison of the pressure tube displacement and the temperatures of the pressure tube and bearing pad. In these figures, the change in the pressure-tube heatup rate is marked with a broken line. Corresponding to the drop in the pressure tube heatup rate, the bearing-pad (TC6) showed an increase in its heatup rate during this time period. At the onset of pressure-tube ballooning, a decrease in pressure-tube heatup rate was an indication of poor physical contact between bearing pad and pressure tube. An increasing bearing-pad heatup rate, simultaneous with the pressure-tube heatup rate decrease, confirmed the deteriorating contact and calculated bearing-pad to pressure-tube heat transfer coefficients reflect this change in the contact geometry after the onset of ballooning. A phenomenological explanation for the reduction in the contact conductance, during the final stages of the bearing-pad to pressure-tube contact heat transfer experiments, will be given in the following section.

3.3.2 Post Ballooning Contact Conductance

The experimental results and subsequent analysis of full scale integrated tests showed the bearing-pad to pressure-tube contact conductance to decrease once the pressure tube began to balloon. For the contact conductance to decrease, the pressure tube must locally strain beneath the bearing pad. Localized deformation under the bearing pad occurs if pressure-tube temperatures exceed temperatures where pressure tube creep become significant. This temperature is deemed the "threshold" temperature for this study. The pressure tube section opposite the bearing-pad ring must reach this threshold temperature sometime earlier than the rest of the pressure tube sections. The time lag for the rest of the pressure-tube sections to reach the threshold temperature must be sufficient for localized ballooning to occur under the bearing pads.

Threshold Temperature

When a thin-walled tube is pressurized internally, hoop stresses (σ_h) develop in the circumferential direction. Typically the hoop stresses are calculated using the following relationship

$$\sigma_h = P D / 2 t \quad (2)$$

where P is the internal pressure, D is the diameter of the tube, and t is the wall thickness of the tube. The pressure tube in a CANDU reactor is designed with a hoop stress well below the yield stress of Zr-2.5 Nb material during normal operating conditions. The yield stress of Zr-2.5 Nb decreases with an increase in temperature [11]. The typical influence of temperature on the yield stress of Zr-2.5 Nb (given in Reference [11]) is shown by the solid line in Figure 5b. In the bearing-pad to pressure-tube experiments the pressure inside the pressure tube ranged between 1 MPa to 6 MPa. During the transient, as the pressure tube temperature rose, the internal hoop stresses did not change in magnitude, but the yield stress of the pressure tube material decreased considerably as shown by the solid line in Figure 5b. For example, in test 11 an internal pressure (gauge) equal to 1.0 MPa induced a hoop stress equal to 12.1 MPa. This hoop stress is marked as point "A" in Figure 5b at room temperature. As the temperature of the pressure tube increased, the path followed by the pressure tube material in test 11 is marked by a horizontal arrow pointing towards the temperature-yield stress curve. When the temperature of the pressure tube was closer to the temperature-yield point curve (threshold temperature) the pressure tube began to deform plastically.

The plastic strain of the pressure tube produced a localized bulge along the diametral axis beneath the bearing pads (Figure 5c). Consequently, the rate of heat transfer through the contact surfaces decreased resulting in a decreased heatup rate of the pressure tube. Logically then, the threshold temperature where the change in pressure tube heatup rate occurred must be relevant to the temperature-yield stress curve shown in Figure 5b. To test this hypothesis the initial hoop stresses of all twelve tests were calculated using Equation 2. These stresses were then located in Figure 5b with the temperatures, corresponding to the inflexion point observed in pressure tube heatup rates. The location where the inflexion point occurred are marked with a broken line in these figures. Satisfactory agreement is shown in Figure 5b between the temperature-yield stress curve of Reference [11] and the pressure-tube heatup-rate inflexion point (which is the threshold temperature). The temperature-yield stress curve (Figure 5b) satisfactorily calculated the threshold temperatures, where pressure tube heatup rate decreased. Thus, the localized bulge in the pressure tube beneath the bearing pad is dependent on a threshold temperature determined by the material properties of Zr-2.5 Nb and the internal pressure of the tube.

4. SUMMARY AND CONCLUSIONS

The integrated bearing-pad to pressure-tube rupture experiments were analysed using CATHENA MOD-3.4b/Rev 7 to infer the bearing-pad to pressure-tube contact conductance transients for the experiment. Ten of these tests used "as received" bearing pads and one test each used a "worn" and a "T-type" bearing pad at the central bottom of the fuel element simulator bundle mounted inside a reactor grade Zr-2.5 Nb pressure tube. The tests were conducted at internal pressures ranging from 1 MPa to 6 MPa. The pressure tube in these tests were filled with two different fluids. The first series (four tests) used steam while the second series (eight tests) used 75% Ar and 25% O₂ gas mixture. From the analysis of integrated tests the following conclusions can be made:

1. Two CATHENA models were developed to derive the bearing-pad to pressure-tube contact conductance using the experimental data. Model A was used to determine the fuel element simulator cladding emissivity transients which were then used in model B to estimate the bearing-pad to pressure-tube contact conductance transients. The present analysis showed this modeling approach provided satisfactory results.
2. The derived bearing-pad to pressure-tube contact conductance showed the following variation during the transient:
 - a) During the initial heatup, the bearing-pad to pressure-tube contact conductance ranged between 0.05 and 2.1 kW/(m² · K) in the Ar/O₂ tests and between 1.1 and 6.8 kW/(m² · K) in the steam tests. The high initial values in steam were attributed to the presence of liquid in the interstitial gap between the bearing pad and the pressure tube.
 - b) The maximum value of bearing-pad to pressure-tube contact conductance in the Ar/O₂ tests during the bulk of the experiment ranged between 1.1 and 1.5 kW/(m² · K), except in one test where a value of 2.0 kW/(m² · K) was reached for a period of 2 s. In the steam tests, the maximum bearing-pad to pressure-tube contact conductance (excluding the initial heatup period) was approximately twice that of the Ar/O₂ tests, i.e. 4.5 kW/(m² · K). These maxima typically occurred when the pressure-tube surface was between 400 °C and 500 °C.
 - c) The contact conductance decreased to a negligible value in all experiments once the pressure tube began to deform due to localized bulging of the pressure-tube under the bearing pads. The threshold temperature for the onset of this bulging was dependent on the internal pressure (hoop stress). The temperature-yield stress relationship satisfactorily calculated this threshold temperature and the onset of pressure-tube ballooning.

REFERENCES

- (1) DEVALL, J.W., M.H. SCHANKULA, V.D. KROEGER, D.B. REEVES, A.P. MUZUMDAR and S.D. SHERIDAN, "An Experimental and Analytical Approach to Determine Bearing-Pad to Pressure-Tube Heat Transfer", Proceedings of the 9th CNS Annual Conference, 1988, pp 110-119.
- (2) MUZUMDAR, A.P., G.R. BERZINS, M. KRAUSE and J.W. DEVALL, "ANSYS Thermal Analysis of Bearing Pad/Pressure Tube Interface", Proceedings of the 3rd International Conference on Simulation Methods in Nuclear Engineering, Montreal, 1990, pp 1055-1075.
- (3) KRAUSE, M., P.M. MATHEW and V.D. KROEGER, "Thermal Analysis of Bearing-Pad to Pressure-Tube Contact Heat Transfer Using ABAQUS", Proceedings of the 4th International Conference on Simulation Methods in Nuclear Engineering, Montreal, Quebec, 1993.
- (4) MOYER, R.G., D.B. SANDERSON, R.W. TIEDE, and H.E. ROSINGER, "Bearing-Pad/Pressure-Tube Rupture Experiments", Proceedings of the 13th CNS Annual Conference, Saint John, New Brunswick, 1992.
- (5) RICHARDS, D.J., B.N. HANNA, N. HOBSON, and K.H. ARDON, "CATHENA: A Two-Fluid Code for CANDU LOCA Analysis, (renamed from ATHENA)", Presented at the 3rd International Topical Meeting on Reactor Thermalhydraulics, Newport, RI, 1985.
- (6) NITHEANANDAN, T., Q.M. LEI, and R.G. MOYER, "Analysis of Bearing-Pad to Pressure-Tube Contact Heat Transfer", Proceedings of the 1994 CNS Simulation Symposium, Pembroke, Ontario, 1994, pp. 274-290.
- (7) SIEGEL, R. and J.R. HOWELL, "Thermal Radiation Heat Transfer", Second Edition, Hemisphere Publishing Corporation, New York, 1981.
- (8) INCROPERA, F.P. and D.P. DEWITT, "Fundamentals of Heat and Mass Transfer", Second Edition, John Wiley and Sons, New York, 1985.
- (9) "Encyclopedia of Chemical Technology", Vol. 23, Weiley Interscience.
- (10) HOHORST, J.K., "CDAP/RELAP5/MOD2 Code Manual, Volume 4: MATPRO - A Library of Materials Properties for Light-Water-Reactor Accident Analysis", Prepared for U.S. Nuclear Regulatory Commission, NUREG/CR-5273, 1990, pp 5.4-1 to 5.4-15.
- (11) ROSINGER, H.E., and A.E. UNGER, "The Superplastic and Strain-Rate Dependent Plastic Flow of Zirconium-2.5 wt.% Niobium in the 873 to 1373 K Temperature Range", Report AECL-6418, December 1979.

TABLE 1
TEST CONDITIONS OF BEARING-PAD TO PRESSURE-TUBE CONTACT HEAT TRANSFER EXPERIMENTS

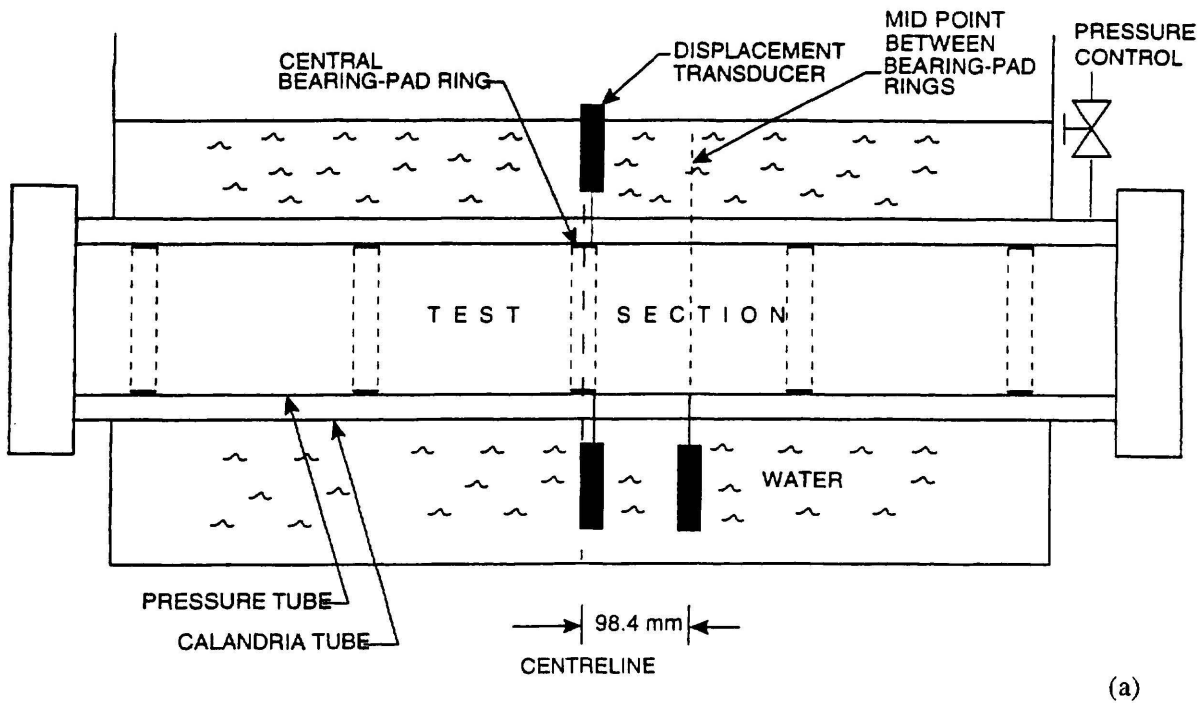
Test No.	Pressure MPa	Fluid	FES Power kW/m	Max. PT Heatup Rate °C/s	Bundle Power kW/m	Temperature at which PT Heatup rate changes °C	Type of Bearing Pad	Rupture
1	2.0-3.0	Steam	4.1	3.4	65.5	638	AR ^a	None
2	3.0-3.5	Steam	8.3	7.6	132	629	AR	None
3	6.0	Steam	5.0	3.8	80	639	AR	None
4	6.0	Steam	8.4	7.4	136	637	AR	None
5	3.0	Ar/O ₂	8.1	7.7	130	667	AR	None
6	6.0	Ar/O ₂	7.7	7.4	123	637	AR	Top ¹
7	3.0	Ar/O ₂	8.1	8.6	130	657	AR	None
8	3.0	Ar/O ₂	8.5	8.2	136	644	worn ^b	None
9	3.0	Ar/O ₂	8.0	8.9	128	658	T ^c	None
10	6.0	Ar/O ₂	8.1	6.3	130	640	AR	Bottom ²
11	1.0	Ar/O ₂	8.2	7.2	131	770	AR	None
12	3.0	Ar/O ₂	10.1	10.1	162	650	AR	Bottom ²

1. Rupture on the top of the Pressure Tube at the central bearing pad location.
 2. Rupture occurred in-between bearing pads at the bottom of the Pressure Tube.
- a. As received Bearing Pads.
 - b. Abraded worn Bearing Pads.
 - c. Modified T type Bearing Pads.

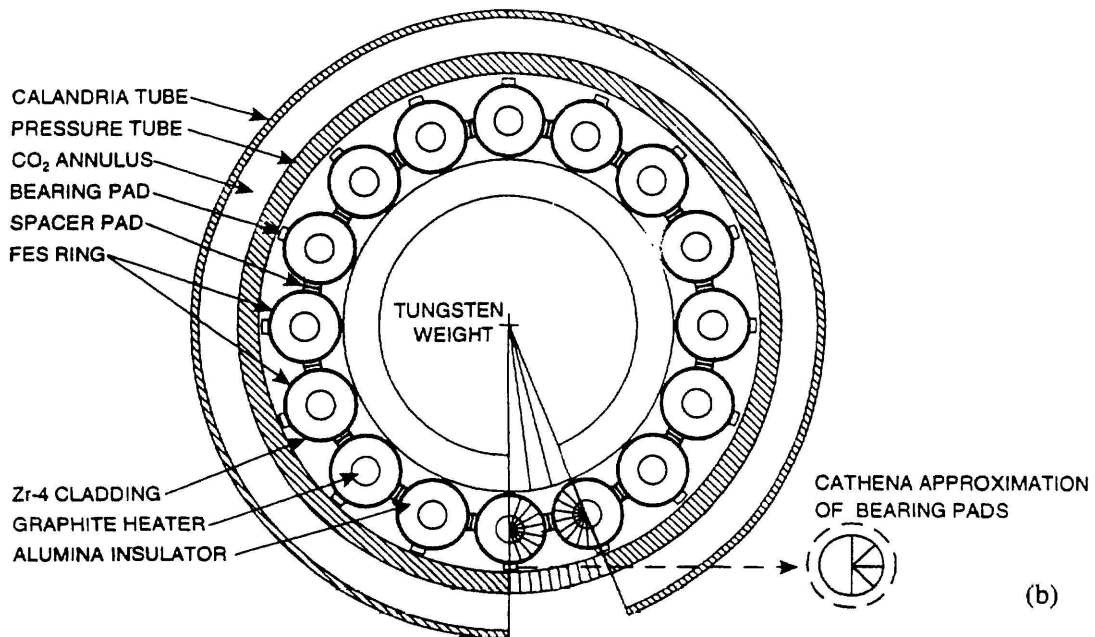
TABLE 2
CALCULATED BEARING-PAD TO PRESSURE-TUBE CONTACT HEAT TRANSFER COEFFICIENTS

Test No.	Test Fluid	Pressure (MPa)	Bearing-Pad to Pressure-Tube Contact Conductance, kW/(m ² ·K)		
			Initial	Maximum	Final
2	Steam	3.0-3.5	6.8 ^a	2.3	< 0.1
3	Steam	6.0	4.4	4.5	< 0.1
4	Steam	6.0	1.1	1.0	< 0.1
5	Ar/O ₂	3.0	0.5	0.5	< 0.1
6	Ar/O ₂	6.0	2.1 ^b	2.0 ^c	< 0.1
7	Ar/O ₂	3.0	0.1	0.5	< 0.1
8	Ar/O ₂	3.0	< 0.1	1.1	< 0.1
9	Ar/O ₂	3.0	0.2	0.8	< 0.1
10	Ar/O ₂	6.0	0.6	0.9	< 0.1
11	Ar/O ₂	1.0	< 0.1	1.0	< 0.1
12	Ar/O ₂	3.0	< 0.1	1.5	< 0.1

- a. Decreased to 3 kW/(m²·K) within 5 s.
- b. Decreased to 1.1 kW/(m²·K) within 5 s.
- c. Remained at 2 kW/(m²·K) for less than 2 s.

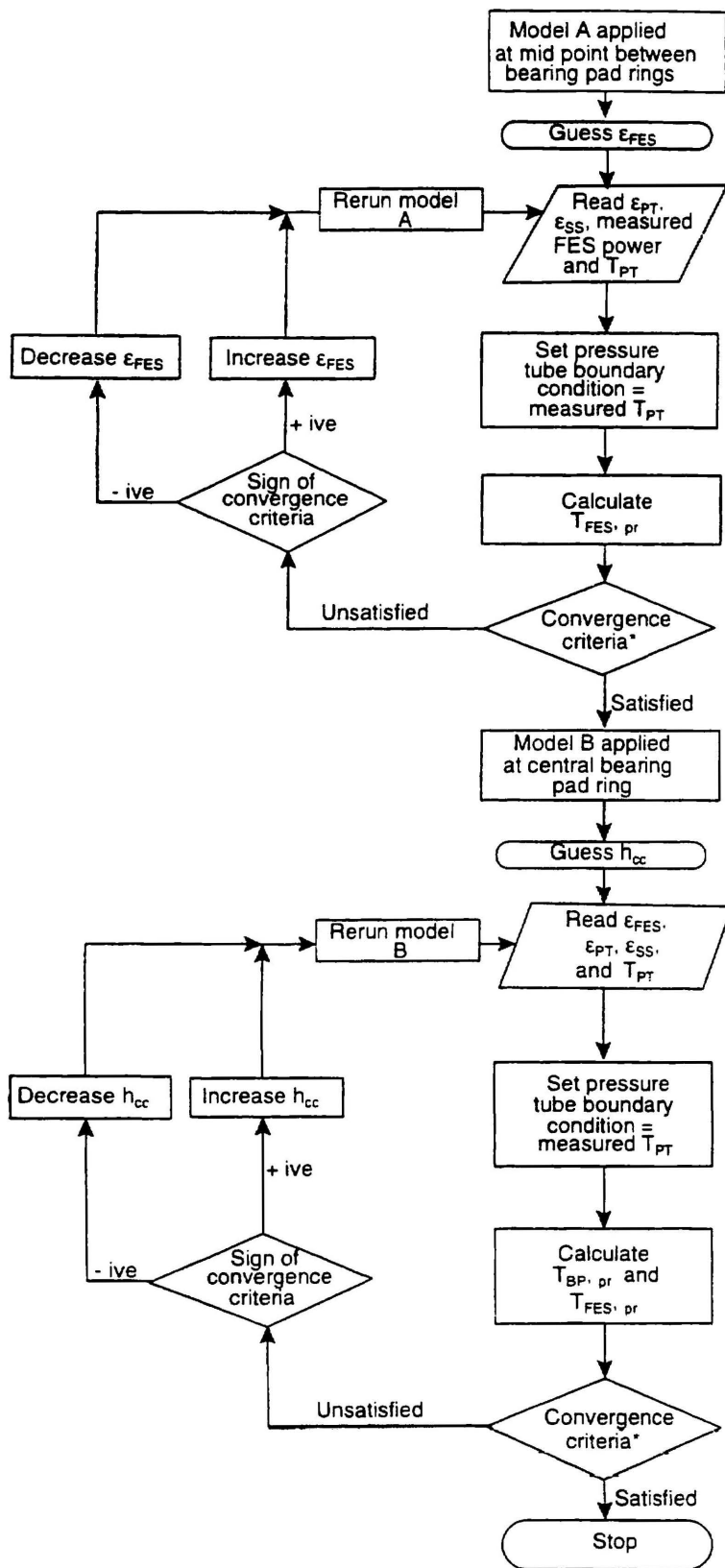


(a)



(b)

FIGURE 1: a) SCHEMATIC OF EXPERIMENTAL APPARATUS AND
b) CROSS-SECTION AT THE CENTRELINE OF THE TEST SECTION SHOWING FES BUNDLE
CONFIGURATION AND CATHENA MODEL SECTORIZATION (BOTTOM RIGHT)



*Convergence criteria = $\frac{T_{exp} - T_{x, pr}}{T_{exp}}$
 where x is $T_{FES, pr}$ in model A and $T_{BP, pr}$ in model B.
 T_{exp} is the measured temperature of corresponding component.

FIGURE 2: PROCEDURE FOLLOWED IN DETERMINING THE CONTACT CONDUCTANCE BETWEEN THE BEARING PAD AND THE PRESSURE TUBE

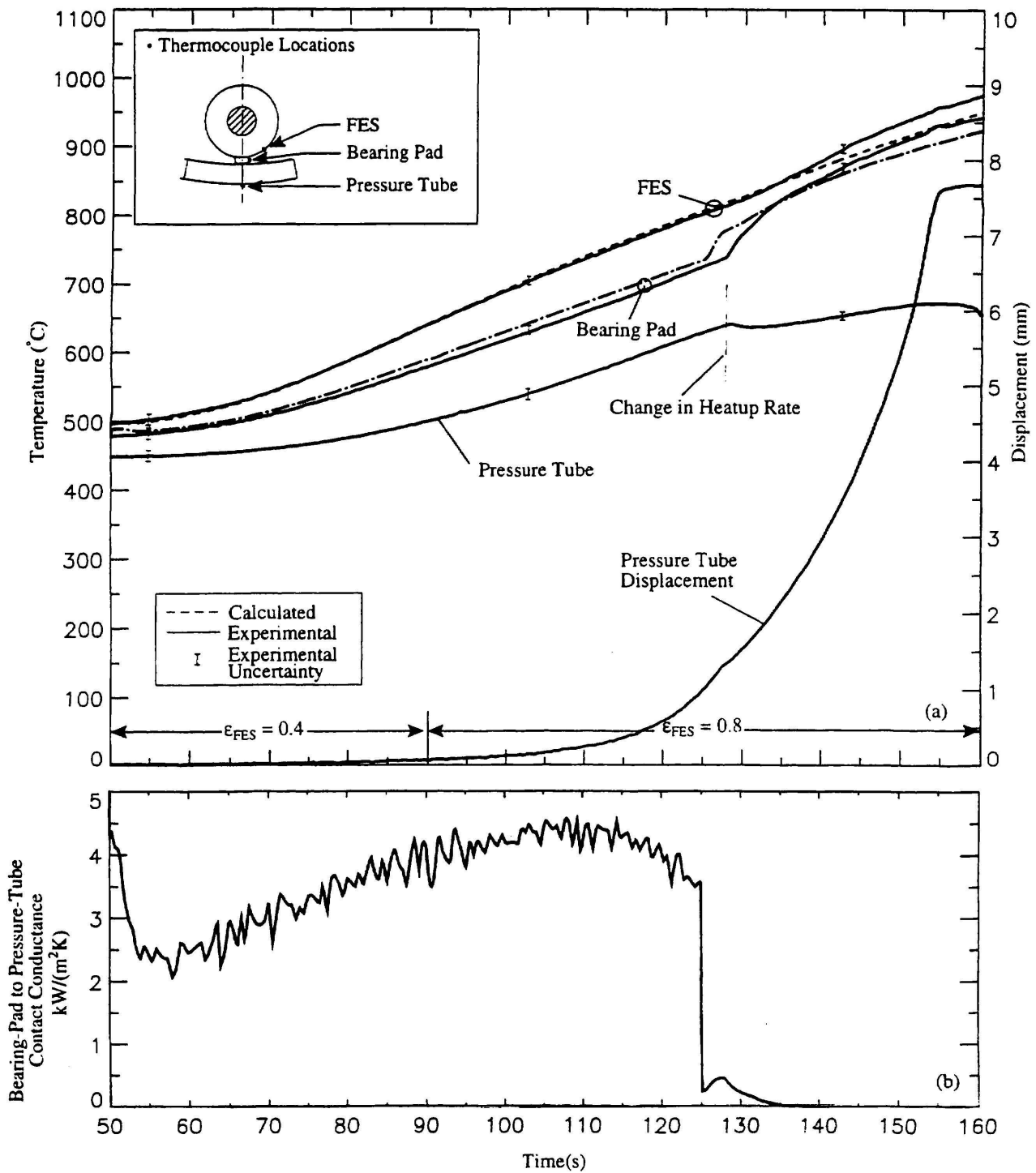


FIGURE 3: a) COMPARISON OF CATHENA CALCULATIONS WITH EXPERIMENTAL DATA
 b) ESTIMATED BOTTOM BEARING-PAD TO PRESSURE-TUBE CONTACT CONDUCTANCE IN TEST 3

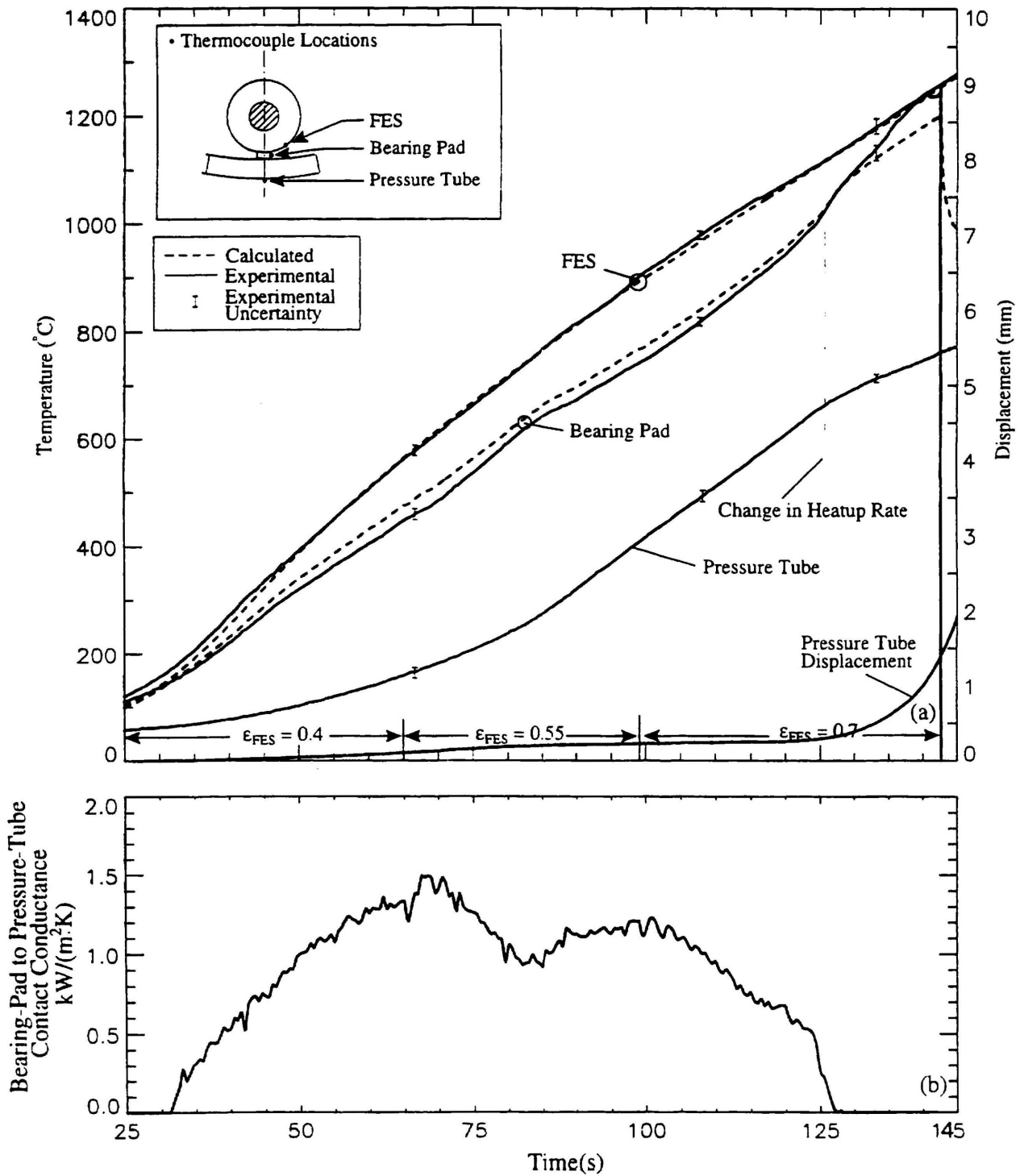


FIGURE 4: a) COMPARISON OF CATHENA CALCULATIONS WITH EXPERIMENTAL DATA
 b) ESTIMATED BOTTOM BEARING-PAD TO PRESSURE-TUBE CONTACT CONDUCTANCE IN TEST 12

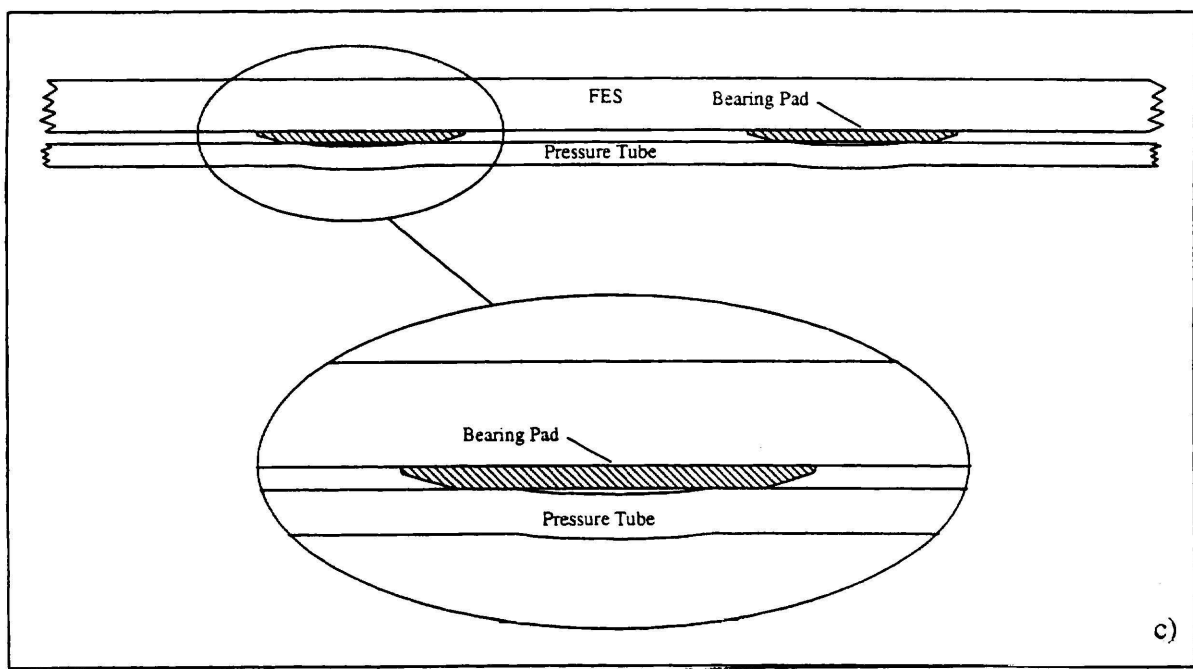
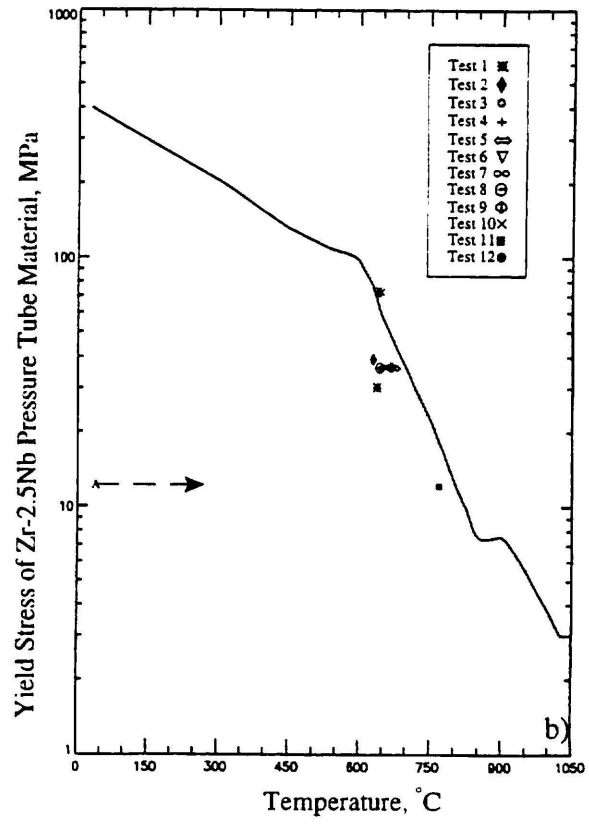
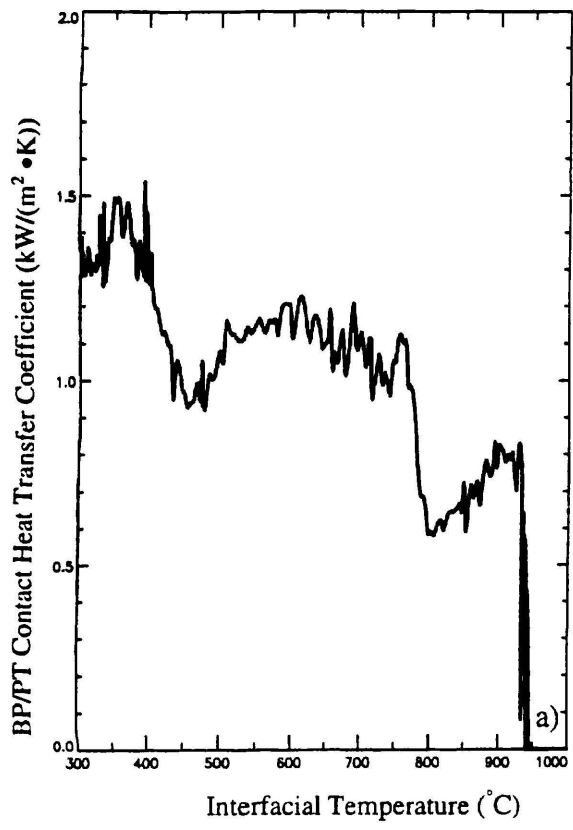


FIGURE 5: a) THE MAXIMUM CONTACT HEAT TRANSFER COEFFICIENTS OBTAINED FROM Ar/O_2 TESTS
 b) THE INFLUENCE OF THRESHOLD TEMPERATURE ON THE YIELD STRESS OF Zr-2.5% Nb PRESSURE-TUBE MATERIAL
 c) THE PRESSURE-TUBE BULGE UNDER THE BEARING PAD